



Contents lists available at ScienceDirect

Journal of King Saud University – Science

journal homepage: www.sciencedirect.com

Original article

Numerical solution for the Kawahara equation using local RBF-FD meshless method

Mohammad Navaz Rasoulizadeh^a, Jalil Rashidinia^{b,*}^aDepartment of Mathematics, Faculty of Basic Sciences, Velayat University, Iranshahr 99111-31311, Iran^bSchool of Mathematics, Iran University of Science and Technology, Narmak, Tehran 16846-13114, Iran

ARTICLE INFO

Article history:

Received 22 July 2019

Revised 17 February 2020

Accepted 2 March 2020

Available online 10 March 2020

Keywords:

Radial basis functions (RBFs)

RBF-FD method

Nonlinear evolution equations

Solitary wave interaction

Kawahara equation

ABSTRACT

When the number of nodes increases more than thousands, the arising system of global radial basis functions (RBFs) method becomes dense and ill-conditioned. To solve this difficulty, local RBFs generated finite difference method (RBF-FD) were introduced. RBF-FD method is based on local stencil nodes and so it has a sparsity system. The main goal in this work is to develop the RBF-FD method in order to obtain numerical solution for the Kawahara equation as a time dependent partial differential equation that appears in the shallow water and acoustic waves in plasma. For this purpose, we have discretized the temporal and spatial derivatives with a finite difference, θ -weighted, and RBF-FD methods. Then by applying the collocation technique at the grid nodes, a system of linear equations is obtained which gives the numerical solution of the Kawahara equation. The stability analysis is given. The efficiency and accuracy of the proposed approach are tested by four examples. In addition, a comparison between proposed method and the methods, RBFs, differential quadrature (DQM), cosine expansion based differential quadrature (CDQ) and modified cubic B-Spline differential quadrature (MCBC-DQM) is shown.

© 2020 The Author(s). Published by Elsevier B.V. on behalf of King Saud University. This is an open access article under the CC BY-NC-ND license (<http://creativecommons.org/licenses/by-nc-nd/4.0/>).

1. Introduction

Nonlinear evolution equations play an essential role in engineering and mathematical physics such as solid state physics, fluid mechanics, chemical physics, plasma physics, geochemistry and chemical kinematics fields (Ablowitz et al., 1991; Jeffrey and Xu, 1989; Raslan and EL-Danaf, 2010; Mohanty and Gopal, 2011; Sharifi and Rashidinia, 2019; Mohanty and Khurana, 2019; Nikan et al., 2019). One of the well-known nonlinear evolution equations is the fifth order Kawahara equation which is appeared in the theories of shallow water waves having surface tension, magneto-acoustic waves in a plasma and capillary-gravity waves (Korkmaz and Dağ, 2009; Sirendaoreji, 2004). In this study, we consider the Kawahara equation (Ceballos et al., 2007) in the following form

$$\frac{\partial V}{\partial t} + \frac{105}{16} \mu^2 V \frac{\partial V}{\partial x} + \frac{13}{4} \rho \frac{\partial^3 V}{\partial x^3} - \frac{\partial^5 V}{\partial x^5} = 0, \quad a \leq x \leq b, \quad 0 < t \leq T, \quad (1a)$$

with the initial condition

$$V(x, 0) = g(x), \quad a \leq x \leq b, \quad (1b)$$

and the boundary conditions

$$\begin{aligned} V(a, t) &= h_a(t), & V(b, t) &= h_b(t), & 0 \leq t \leq T, \\ V_x(a, t) &= V_x(b, t) = V_{xx}(b, t) = 0, & 0 \leq t \leq T. \end{aligned} \quad (1c)$$

Where $V = V(x, t)$; and g, h_a, h_b are known functions and μ and ρ are known coefficients.

In special forms of the Kawahara equation, the analytical solution in the case of solitary waves is studied by some researchers (Sirendaoreji, 2004; Yamamoto and Takizawa, 1981; Yusufoglu et al., 2008). Generally, obtaining the analytic solution for the nonlinear differential equations is not possible, so the numerical approximations are necessary for solving such models (Bashan et al., 2017; Başhan, 2019; Başhan, 2019). The numerical solution of the Kawahara equation has been investigated by many researchers (Korkmaz and Dağ, 2009; Djidjeli et al., 1995; Ceballos et al., 2007; Haq and Uddin, 2011; Abazari and Soltanalizadeh, 2012; Gong et al., 2014; Karakoc et al., 2014; Başhan, 2019). Also, some other methods based on homotopy analysis are proposed for the approximate solution of the Kawahara equation (Abbasbandy, 2010; Wang, 2011; Kashkari, 2014).

In recent years, RBFs meshfree collocation techniques have been extensively used for obtaining the numerical solutions of PDEs (Sarra, 2005; Meshfree, 2007; Hussain and Haq, 2020; Dereli

* Corresponding author.

E-mail addresses: mnrasoulizadeh@gmail.com (M.N. Rasoulizadeh), rashidinia@iust.ac.ir (J. Rashidinia).

et al., 2009; Bibi et al., 2011; Safdari-Vaighani and Mahzarnia, 2015). Some of the major advantages of RBFs approaches are spectral convergence rates, computing derivatives, geometrical flexibility and the ease of applying in high dimensions. Although RBFs methods have a spectral accuracy, they often have a large linear system with full and ill-conditioned matrices. To overcome such difficulties, the local RBF-FD method was investigated by some authors (Wright and Fornberg, 2006; Bayona et al., 2010; Martin and Fornberg, 2017; Dehghan and Mohammadi, 2017; Dehghan and Abbaszadeh, 2017; Nikan et al., 2019; Rashidinia and Rasoulizadeh, 2019). This method has a sparse and well-conditioned system.

The main purpose of this manuscript is to develop the local RBF-FD method to solve the Kawahara equation as a time-dependent PDEs. In addition, a comparison between proposed method and the methods MQ and r^7 RBFs (Haq and Uddin, 2011), CDQ and PDQ (Korkmaz and Dağ, 2009), and MCBC-DQM (Başhan, 2019) is given.

The rest of the present study is as follows; In Section 2, the RBFs and RBF-FD collocation methods will be reviewed briefly. In Section 3, a description of the meshless RBF-FD method to compute the numerical solution of the Kawahara equation is given. In Section 4, the stability analysis of the proposed method is proved. In Section 5, the numerical experiments is reported.

2. Collocation methods

Let $X = \{\underline{x}_1, \underline{x}_2, \dots, \underline{x}_N\} \subseteq \mathbb{R}^d$, be a set of N separate points with known scalar values f_i for $i = 1, 2, \dots, N$.

2.1. RBF collocation method

RBF interpolation is defined as

$$s(\underline{x}, \varepsilon) = \sum_{j=1}^N \lambda_j \phi_j(\underline{x}),$$

where $\phi_j(\underline{x}) = \phi(\|\underline{x} - \underline{x}_j\|, \varepsilon)$, $\|\cdot\|$ is the Euclidean norm, ε is the shape parameter and ϕ is a radial function. To determine $\{\lambda_j\}_{j=1}^N$, the collocation method is used.

$$s(\underline{x}_i, \varepsilon) = f_i, \quad i = 1, \dots, N. \quad (3)$$

The Eq. (3) leads to a linear system of equations as

$$A_\phi \lambda = f, \quad (4)$$

where

$$\lambda = \begin{bmatrix} \lambda_1 \\ \lambda_2 \\ \vdots \\ \lambda_N \end{bmatrix}, \quad f = \begin{bmatrix} f_1 \\ f_2 \\ \vdots \\ f_N \end{bmatrix}, \quad A_{\phi,ij} = \phi_j(\underline{x}_i), \quad i, j = 1, \dots, N.$$

The non-singularity of the matrix A_ϕ for some RBFs was proved by Micchelli (Micchelli, 1984).

2.2. RBF-FD collocation method

Suppose $I_i = \{\underline{x}_{i_1}, \underline{x}_{i_2}, \dots, \underline{x}_{i_{n_i}}\}$ be a stencil of \underline{x}_i and \mathcal{L} be a linear differential operator. We want to find $w = (w_1, w_2, \dots, w_{n_i})$ such that

$$\mathcal{L} u(\underline{x}_i) = \sum_{j=1}^{n_i} w_j u(\underline{x}_{i_j}), \quad (5)$$

where $\underline{x}_i = \underline{x}_{i_1}$ is the center node of stencil I_i . By using $\phi_j(x) = \phi(\|\underline{x} - \underline{x}_j\|)$, $j = 1, \dots, n_i$, instead of $u(x)$ in Eq. (5), the weights can be computed from the following system:

$$A_\phi w = l, \quad (6)$$

where

$$w = \begin{bmatrix} w_1 \\ w_2 \\ \vdots \\ w_{n_i} \end{bmatrix}, \quad l = \begin{bmatrix} \mathcal{L} \phi_{i_1}(\underline{x})|_{\underline{x}=\underline{x}_i} \\ \mathcal{L} \phi_{i_2}(\underline{x})|_{\underline{x}=\underline{x}_i} \\ \vdots \\ \mathcal{L} \phi_{i_{n_i}}(\underline{x})|_{\underline{x}=\underline{x}_i} \end{bmatrix}, \quad A_{\phi,rs} = \phi_{i_r}(\underline{x}_s), \quad r, s = 1, \dots, n_i. \quad (7)$$

The weights w_1, w_2, \dots, w_{n_i} can be determined from the above system. Furthermore, the convergence analysis of RBF-FD formula, Eq. (5), have been proved analytically by Bayona, Moscoso and et al., (Bayona et al., 2010).

3. Description of the method

The implementation details of the RBF-FD method for the Kawahara equation are described in this section.

First, $m + 1$ distinct points $t_k = k\tau$, $k = 0, 1, \dots, m$, on interval $[0, T]$ with time step size τ are chosen. Then, the finite difference (FD) and θ -weighted ($0 \leq \theta \leq 1$) methods are applied over two consecutive time steps t_k and t_{k+1} on Eq. (1) as

$$\frac{V^{k+1} - V^k}{\tau} + \theta \left(\frac{105}{16} \mu^2 V \frac{\partial V}{\partial x} + \frac{13}{4} \rho \frac{\partial^3 V}{\partial x^3} - \frac{\partial^5 V}{\partial x^5} \right)^{k+1} + (1 - \theta) \left(\frac{105}{16} \mu^2 V \frac{\partial V}{\partial x} + \frac{13}{4} \rho \frac{\partial^3 V}{\partial x^3} - \frac{\partial^5 V}{\partial x^5} \right)^k = 0, \quad (8)$$

where $k = 0, 1, \dots, (m - 1)$, $V^k = V(x, t_k)$ and $V^{k+1} = V(x, t_{k+1})$.

The nonlinear term $(V \frac{\partial V}{\partial x})^{k+1}$ can be approximated by linear term (Rashidinia and Rasoulizadeh, 2019) as

$$\left(V \frac{\partial V}{\partial x} \right)^{k+1} = V^k \frac{\partial V^{k+1}}{\partial x} + V^{k+1} \frac{\partial V^k}{\partial x} - V^k \frac{\partial V^k}{\partial x}. \quad (9)$$

After substituting Eq. (9) into Eq. (8), it can be written as

$$\begin{aligned} & \left(1 + \frac{105}{16} \theta \tau \mu^2 V_x^k \right) V^{k+1} + \theta \tau \left(\frac{105}{16} \mu^2 V^k V_x^{k+1} + \frac{13}{4} \rho V_{3x}^{k+1} - V_{5x}^{k+1} \right) \\ & = (2\theta - 1) \tau \frac{105}{16} \mu^2 V^k V_x^k - (1 - \theta) \tau \left(\frac{13}{4} \rho V_{3x}^k - V_{5x}^k \right), \quad \text{for } x \in (a, b). \end{aligned} \quad (10)$$

Now, N distinct collocation nodes $X = \{x_1, x_2, \dots, x_N\}$ are chosen in the interval $[a, b]$ in which x_i , $i = 2, \dots, N - 1$ are the $N - 2$ interior nodes and x_i , $i = 1, N$ are the 2 boundary nodes.

For each point x_i , stencil $I_i = \{x_j \in X : |x_j - x_i| \leq R\} = \{x_{i_1}, x_{i_2}, \dots, x_{i_{n_i}}\}$ in its support radius R is chosen. Without loss of generality, let us assume $x_i = x_{i_1}$ ($i = i_1$). For each node x_i and its stencil I_i , the weights $w_{sx,i} = [w_{sx,i,1}, \dots, w_{sx,i,n_i}]^T$ corresponding to $\frac{\partial^s}{\partial x^s}$ for $s = 1, 3$, and 5 will be determined by using RBF-FD method Eq. (6). Thus we obtain

$$V_{sx,i} = V_{sx}(x_i) = \frac{\partial^s V(x_i)}{\partial x^s} = \sum_{j=1}^{n_i} w_{sx,ij} V_{ij}, \quad i = 2, \dots, N - 2, \quad s = 1, 3, 5, \quad (11)$$

where $V_{ij} = V(x_{ij}, t)$. The weights $w_{sx,ij}$ are only dependent on stencil nodes and are independent from the time steps t_k . Applying the

collocation methods on interior nodes in Eq. (10) and using Eq. (11) concluded that

$$\begin{aligned} & \left\{ 1 + \theta \tau \left(\frac{105}{16} \mu^2 (C_{x,i}^k + V_i^k w_{x,i1}) + \frac{13}{4} \rho w_{3x,i1} - w_{5x,i1} \right) \right\} V_i^{k+1} \\ & + \theta \tau \sum_{j=2}^{n_i} \left(\frac{105}{16} \mu^2 V_i^k w_{x,ij} + \frac{13}{4} \rho w_{3x,ij} - w_{5x,ij} \right) V_j^{k+1} \\ & = \left(1 + (2\theta - 1) \tau \frac{105}{16} \mu^2 C_{x,i}^k \right) V_i^k - (1 - \theta) \tau \left(\frac{13}{4} \rho C_{3x,i}^k - C_{5x,i}^k \right), \\ & i = 2, \dots, N-1, \end{aligned} \quad (12)$$

in which $C_{sx,i}^k = \sum_{j=1}^{n_i} w_{sx,ij} V_j^k$ for $s = 1, 3$, and 5 .

Eq. (12) along with the boundary conditions Eq. (1c), lead to the following $N \times N$ linear system of equations with the matrix form as:

$$AV^{k+1} = b, \quad k = 0, 1, \dots, m-1, \quad (13)$$

where $V^{k+1} = [V_1^{k+1}, V_2^{k+1}, \dots, V_N^{k+1}]^t$ is the unknown vector that should be computed. According to Eq. (12), the elements of the sparse matrix $A_{N \times N}$ and vector $b_{N \times 1}$ are as follows:

$$\begin{aligned} A_{ii} &= 1 + \theta \tau \left(\frac{105}{16} \mu^2 (C_{x,i}^k + V_i^k w_{x,i1}) + \frac{13}{4} \rho w_{3x,i1} - w_{5x,i1} \right), \\ i &= 2, \dots, N-1, \\ A_{ij} &= \frac{105}{16} \mu^2 V_i^k w_{x,ij} + \frac{13}{4} \rho w_{3x,ij} - w_{5x,ij}, \quad i = 2, \dots, N-1, \\ j &= 1, \dots, n_i, \\ A_{11} &= 1, \quad A_{NN} = 1, \quad b_1 = h_a(t_{k+1}), \quad b_N = h_b(t_{k+1}), \\ b_i &= \left(1 + (2\theta - 1) \tau \frac{105}{16} \mu^2 C_{x,i}^k \right) V_i^k - (1 - \theta) \tau \left(\frac{13}{4} \rho C_{3x,i}^k - C_{5x,i}^k \right), \\ i &= 2, \dots, N-1. \end{aligned} \quad (14)$$

The other elements of matrix A are equal zero.

At time level $t_0 = 0$ the value of V^0 can be computed from initial condition Eq. (1b) then by using Eq. (13) the value of V^k at every time step t_k can be computed.

4. Stability analysis

The stability of the proposed method will be analyzed by applying the Von-Neumann linear stability analysis. Although, the Von-Neumann stability analysis is applicable to linear difference equations, it can provide the necessary condition and can be effective in practice for the nonlinear (linearized) difference equation (see (Mokhtari and Mohseni, 2012) and references therein).

For this goal, at first, one variable in the nonlinear terms in Eq. (10) should be locally freezes, i.e., $V^k = u$ and $V_x^k = u_x$, in which u is a locally constant value of V^k and u_x is a locally constant value of V_x^k , then Von-Neumann analysis employed to determine the necessary condition for the stability.

After locally freezing the nonlinear terms $V^k = u$ and $V_x^k = u_x$ in Eq. (10), it can be written as

$$\begin{aligned} & \left(1 + \frac{105}{16} \theta \tau \mu^2 u_x \right) V^{k+1} + \theta \tau \left(\frac{105}{16} \mu^2 u \frac{\partial}{\partial x} V^{k+1} + \frac{13}{4} \rho \frac{\partial^3}{\partial x^3} V^{k+1} - \frac{\partial^5}{\partial x^5} V^{k+1} \right) \\ & = (2\theta - 1) \tau \frac{105}{16} \mu^2 u \frac{\partial}{\partial x} V^k - (1 - \theta) \tau \left(\frac{13}{4} \rho \frac{\partial^3}{\partial x^3} V^k - \frac{\partial^5}{\partial x^5} V^k \right). \end{aligned} \quad (15)$$

Employing the von Neumann's approach by taking $V_j^k = \xi^k e^{ipx_j}$ for each point x_j and substituting it in Eq. (15), we obtain

$$\begin{aligned} & \left(1 + \frac{105}{16} \theta \tau \mu^2 u_x \right) \xi^{k+1} e^{ipx_j} \\ & + \theta \tau \left(\frac{105}{16} \mu^2 u (i\eta) \xi^{k+1} e^{ipx_j} + \frac{13}{4} \rho (i\eta)^3 \xi^{k+1} e^{ipx_j} - (i\eta)^5 \xi^{k+1} e^{ipx_j} \right) \\ & = (2\theta - 1) \tau \frac{105}{16} \mu^2 u (i\eta) \xi^k e^{ipx_j} - (1 - \theta) \tau \left(\frac{13}{4} \rho (i\eta)^3 \xi^k e^{ipx_j} - (i\eta)^5 \xi^k e^{ipx_j} \right). \end{aligned} \quad (16)$$

Above equation concluded that

$$\xi = \frac{(2\theta - 1) \sigma_2 u \eta i + (1 - \theta) \sigma_1 i}{(1 + \theta \sigma_2 u_x) + \theta \sigma_2 u \eta i - \theta \sigma_1 i}, \quad (17)$$

where

$$\sigma_1 = \eta^3 \left(\frac{13}{4} \rho + \eta^2 \right) \tau, \quad \sigma_2 = \frac{105}{16} \mu^2 \tau. \quad (18)$$

Thus

$$|\xi|^2 = \frac{(2\theta - 1) \sigma_2 u \eta + (1 - \theta) \sigma_1^2}{(1 + \theta \sigma_2 u_x)^2 + (\theta \sigma_2 u \eta - \theta \sigma_1)^2} = \frac{G}{H}.$$

We know that if $H - G \geq 0$ then $|\xi| \leq 1$ and the method is stable. By choosing $2\theta - 1 = \theta - (1 - \theta)$ in the above equation and simplifying, we get

$$\begin{aligned} H - G &= 1 + (2\theta - 1) \sigma_1^2 + (1 - \theta)(3\theta - 1)(\sigma_2 u \eta)^2 \\ &+ (\theta \sigma_2 u_x)^2 + 2(\theta^2 - 3\theta + 1) \sigma_1 \sigma_2 u \eta + 2\theta \sigma_2 u_x. \end{aligned} \quad (19)$$

For $\theta = \frac{1}{2}$, the famous Crank-Nicolson (C-N) method, Eq. (19) can be simplified as

$$H - G = (1 + 0.5 \sigma_2 u_x)^2 + (0.5 \sigma_2 u \eta)^2 - 0.5 \sigma_1 \sigma_2 u \eta.$$

Since $\lim_{\tau \rightarrow 0} (0.5 \sigma_1 \sigma_2 u \eta) = 0$, so we can ignore this term in Eq. (20) for enough small values of τ . Therefore, Eq. (20) yields $H - G > 0$ and $|\xi| < 1$, and the proposed method is stable.

5. Numerical experiments

The RBF-FD method is applied for obtaining the numerical solution of the Kawahara equation. The efficiency of the proposed method and convergence order and invariants I_1 and I_2 are tested in terms of the following norms:

1. $L_\infty = \|V^e - V\|_\infty = \max_{1 \leq i \leq N} |V_i^e - V_i|,$
2. $L_2 = \left(\frac{1}{N} \sum_{i=1}^N (V_i^e - V_i)^2 \right)^{\frac{1}{2}},$
3. $C_t - \text{order} = \frac{\log(\frac{E_j}{E_{j+1}})}{\log(\frac{T_j}{T_{j+1}})}, \quad C_x - \text{order} = \frac{\log(\frac{E_j}{h_j})}{\log(\frac{h_j}{h_{j+1}})},$
4. $I_i = \frac{1}{l} \int_a^b V^i dx, \quad i = 1, 2,$

where V^e and V are the exact and computational values of $V(x, t)$ respectively and E_j is the L_2 error with respect to T_j or h_j .

The Matlab software and the kd-tree package (Matlab, 2004) for finding stencils are used to apply RBF-FD method. Moreover, we use $\theta = \frac{1}{2}$, and MQ and TPS RBFs in all examples.

Example 1. For the first example, we consider traveling solitary wave problem of Eq. (1)(refk11) whose exact solution is as follows (Yamamoto and Takizawa, 1981)

$$V(x, t) = \left(\frac{\rho}{\mu} \right)^2 \operatorname{sech}^4 \left(\frac{\sqrt{\rho}}{4} \left(x - x_0 - \frac{36}{169} t \right) \right).$$

Two type RBFs, the shape parameter dependent MQ-RBF, $\Phi(r) = \sqrt{1 + (\epsilon r)^2}$, and the shape parameter independent TPS-RBF, $\Phi(r) = r^4 \log r$, are used to obtain numerical solution of this example. This example is solved in the temporal interval $[0, 30]$ and spatial interval $[-20, 30]$ and the parameters

$\mu = \sqrt{16/105}$, $\rho = 4/13$ and $x_0 = 2$ are chosen. In the Tables 1 and 2, the L_2 , L_∞ error norms and computational order due to the spatial and temporal directions at $T = 1$ are listed. These Tables show that by decreasing spatial and temporal step size, h and τ , the accuracy increases. Table 3 shows that by increasing the number of nodes stencil, n_s , the accuracy increases also. To compare the proposed method with some recent methods, in the Table 4 the L_2 error norms at some time levels of RBF-FD, MQ and r^7 RBF (Haq and Uddin, 2011), CDQ and PDQ (Korkmaz and Dağ, 2009), and MCBC-DQM (Başhan, 2019) methods are reported. It is clear from the Table 4 that the results of RBF-FD methods are better than the other mentioned methods. In the Fig. 1, panels (A) and (B), the graphs of approximation values and absolute point wise error are plotted. Moreover in the Fig. 1 panel (C) the traveling of the single solitary wave at different times is shown. Therefore, these tables and figures confirm the accuracy and efficiency of the proposed method and its improvement versus the earlier above mentioned methods.

Example 2. In this example, the interaction of two solitary waves with the following initial condition is considered

$$V(x, 0) = \sum_{i=1}^2 d_i^2 \operatorname{sech}^4 \left(\frac{\sqrt{\mu d_i}}{4} (x - x_i) \right).$$

This equation is the sum of two solitary waves that are located at $x_1 = 0$ and $x_2 = 20$. For $-50 \leq x \leq 100$, $0 \leq t \leq 50$, $\mu = \sqrt{16/105}$, $\rho_i = (12 - 2i)/13$, $d_i = \rho_i/\mu$, $i = 1, 2$. It is solved by using RBF-FD method with $\tau = 0.01$, $h = 0.2$ and $\epsilon = 1$. The propagating of both waves toward the right is shown in Fig. 2. Also, the two invariants I_1 and I_2 are preserved constant laws as it shown in the Table 5.

Example 3. Here, the interaction of three solitary waves with the following initial condition is considered

Table 1
Error and C_x – order with $\tau = 0.01$ and $n_s = 50$ at $T = 1$ for Example 1.

h	MQ-RBF, $\epsilon h = 0.2$			TPS-RBF		
	L_∞	L_2	C_x – order	L_∞	L_2	C_x – order
2/5	1.7889e – 03	4.0303e – 04	–	1.5236e – 03	3.9466e – 04	–
1/5	6.2189e – 04	1.4499e – 04	1.4749	7.7158e – 04	1.8762e – 04	1.6043
1/10	7.5166e – 05	1.8497e – 05	2.9706	1.5938e – 04	5.2543e – 05	0.8026
1/15	5.9090e – 05	1.5413e – 05	0.4498	1.1487e – 04	3.7814e – 05	1.1381
1/20	3.4884e – 05	1.1860e – 05	0.9109	9.6544e – 05	3.2989e – 05	0.9161
1/25	2.0794e – 05	7.7545e – 06	1.9041	8.7701e – 05	3.1535e – 05	1.0698

Table 2
Error and C_t – order with $h = 0.2$ and $n_s = 50$ at $T = 1$ for Example 1.

τ	MQ-RBF, $\epsilon = 1$			TPS-RBF		
	L_∞	L_2	C_t – order	L_∞	L_2	C_t – order
1/10	6.1666e – 03	2.0797e – 03	–	2.0675e – 03	8.7495e – 04	–
1/20	9.2686e – 04	5.4222e – 04	0.9318	1.0727e – 03	4.5004e – 04	0.9591
1/40	6.3848e – 04	1.4557e – 04	0.9115	7.4467e – 04	2.6368e – 04	0.7713
1/80	6.4189e – 04	1.4495e – 04	0.0062	7.6434e – 04	2.0098e – 04	0.3917
1/160	6.3317e – 04	1.4483e – 04	0.0012	7.6796e – 04	1.8711e – 04	0.1032
1/320	6.2474e – 04	1.4471e – 04	0.0012	7.7001e – 04	1.8598e – 04	0.0087

Table 3
Condition number and errors of Example 1 with $h = 0.1$, $\tau = 0.001$ at $T = 1$ for some values of n_s .

n_s	MQ-RBF, $\epsilon = 2$			TPS-RBF		
	L_∞	L_2	$C(A)$	L_∞	L_2	$C(A)$
10	3.7123e – 02	1.5091e – 02	8.3928e + 04	5.6049e – 04	1.7758e – 04	4.0241e + 03
20	9.9687e – 03	3.2889e – 03	8.3791e + 04	2.5196e – 04	7.6178e – 05	3.5221e + 03
30	9.0622e – 04	3.2028e – 04	8.3413e + 04	1.9234e – 04	5.9022e – 05	3.3753e + 03
40	6.8851e – 05	2.6532e – 05	8.2845e + 04	1.6957e – 04	5.3450e – 05	3.3153e + 03
50	7.4737e – 05	1.8527e – 05	8.2825e + 04	1.5938e – 04	5.2543e – 05	3.2910e + 03

Table 4
Comparison of L_2 error between presented method with $h = 0.1$, $\epsilon = 2$, $n_s = 50$ and $\tau = 0.01$, and the methods MQ and r^7 RBFs (Haq and Uddin, 2011), CDQ and PDQ (Korkmaz and Dağ, 2009), and MCBC-DQM (Başhan, 2019) for Example 1.

t	RBF-FD(MQ)	MQ	r^7	CDQ	PDQ	MCBC-DQM
1	1.8497e – 05	2.387e – 05	2.574e – 05	–	–	–
2	2.1989e – 05	3.585e – 05	2.669e – 04	–	–	–
5	2.4936e – 05	6.278e – 05	2.348e – 02	1.59e – 04	1.986e – 03	6.3e – 05
10	2.9511e – 05	7.692e – 05	–	–	–	6.7e – 05
15	3.3586e – 05	4.466e – 05	–	1.56e – 04	2.543e – 03	5.6e – 05
20	4.1246e – 05	1.344e – 05	–	–	–	6.3e – 05
25	5.0771e – 05	9.370e – 05	–	1.59e – 04	2.851e – 03	7.2e – 05

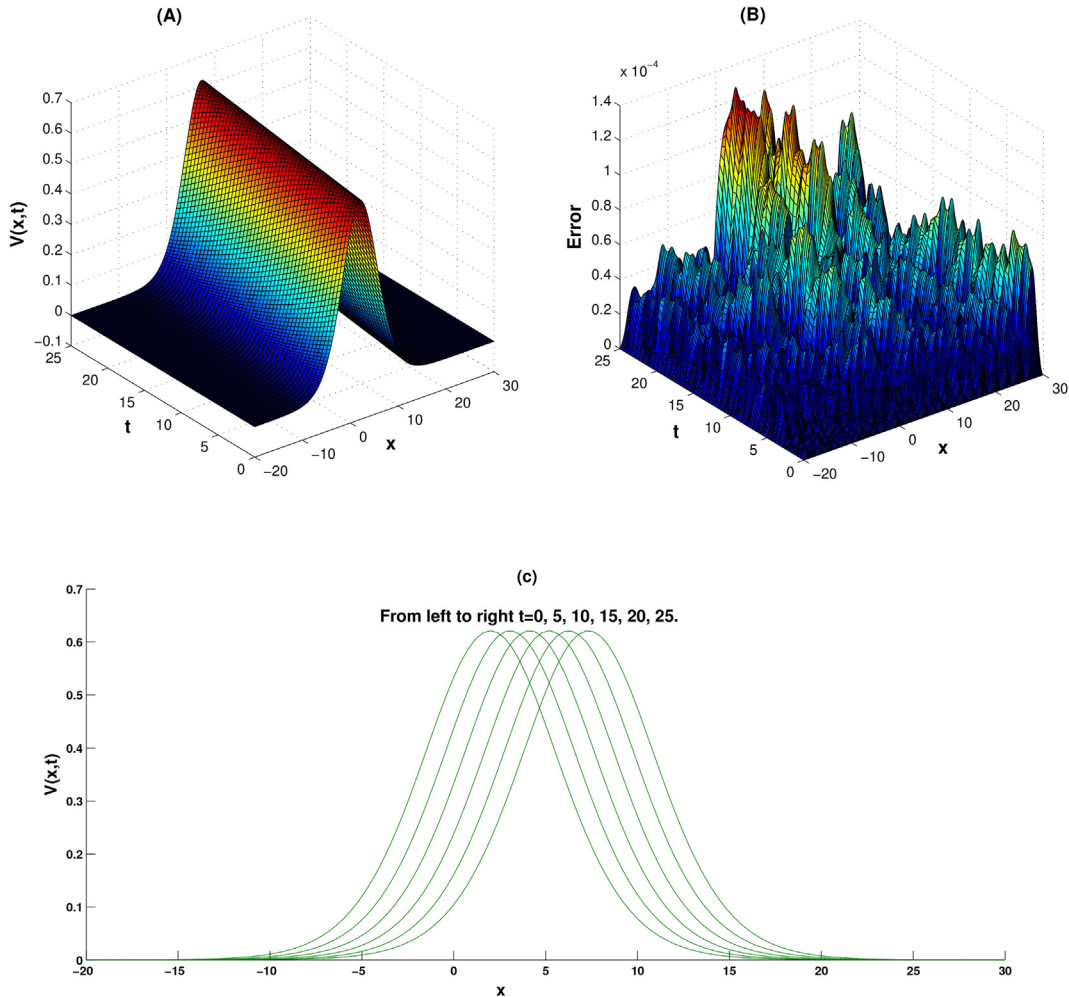


Fig. 1. Graphs of approximation solutions (A) and errors (B), and plots of $V(x, t)$ at $t = 0, 5, 10, 15, 20, 25$ (C), using the RBF-FD method with $\epsilon = 2$, $h = 1/10$, $n_s = 50$ and $\tau = 1/100$ for Example 1.

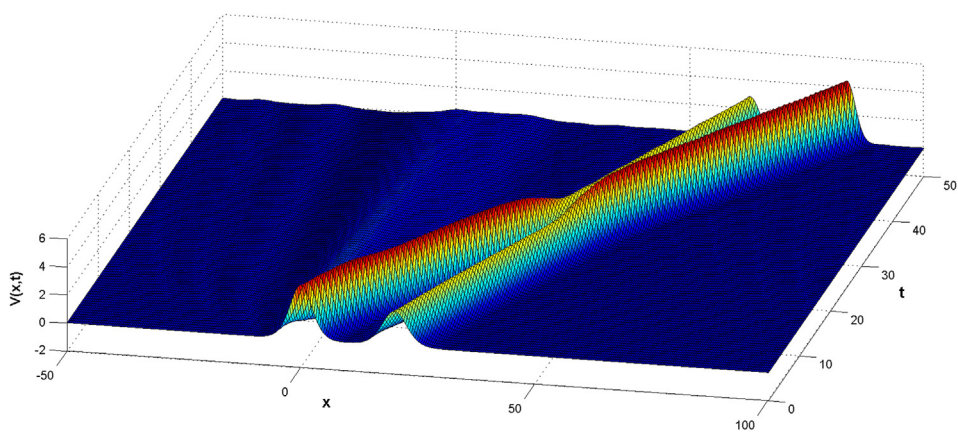


Fig. 2. Graphs of approximation solutions using the RBF-FD method with $\epsilon = 2$, $h = 1/10$, $n_s = 50$ and $\tau = 1/100$ for Example 2.

$$V(x, 0) = \sum_{i=1}^3 d_i^2 \operatorname{sech}^4 \left(\frac{\sqrt{\mu d_i}}{4} (x - x_i) \right).$$

This equation is the sum of three solitary waves that are located at $x_1 = -20$, $x_2 = 0$ and $x_3 = 20$. For $-30 \leq x \leq 120$, $0 \leq t \leq 60$, $\mu = \sqrt{16/105}$, $\rho_i = (12 - 2i)/13$, $d_i = \rho_i/\mu$, $i = 1, 2, 3$,

it is solved using RBF-FD method with $\tau = 0.01$, $h = 0.2$, $n_s = 50$ and $\epsilon = 1$. The motion of three waves from the left to the right is shown in Fig. 3.

Example 4. In this example a type of the Kawahara Eq. (1) in the following form is considered,

$$V_t + VV_x + V_{3x} + V_x - V_{5x} = 0,$$

in which, the exact solitary wave solution is given (Ceballos et al., 2007) as

Table 5

Invariants of proposed method and RBF method (Haq and Uddin, 2011) for Example 2 with $h = 0.2$, $\epsilon = 1$ and $\tau = 0.01$, and MQ.

Time	RBF-FD		RBF	
	I_1	I_2	I_1	I_2
0	40.5093	45.8361	40.50926	45.83614
5	40.4693	45.8361	40.50690	45.83557
20	40.4416	45.8360	40.53983	45.83547
30	40.5631	45.8361	40.46771	45.83544
40	40.4567	45.8362	40.58194	45.83535
55	40.4686	45.8366	40.40483	45.83524

$$V(x, t) = \frac{105}{169} \operatorname{sech}^4 \left(\frac{1}{2\sqrt{13}} \left(x - x_0 - \frac{205}{169} t \right) \right).$$

This example also has been solved by RBF-FD method. The graphs of approximation solution and point wise error, and the interaction profile of single solitary wave with $\tau = 0.001$, $h = 0.1$, $\epsilon = 2$, $n_s = 50$ on region $(x, t) \in [-20, 50] \times [0, 60]$ has been shown in Fig. 4. In the Table 6, a comparison of the error norms L_2 and L_∞ , and invariants I_1 and I_2 between proposed method and RBFs method (Haq and Uddin, 2011) is reported. From this table it is clear that the presented method has a good agreement with the exact result and has a better accuracy than the RBF method (Haq and Uddin, 2011). Also, the respected changes of invariants I_1 and I_2 of RBF-FD method are approximately constant and acceptable. Furthermore, the condition number of the RBF-FD method is equal to $5.9063e + 04$ and the

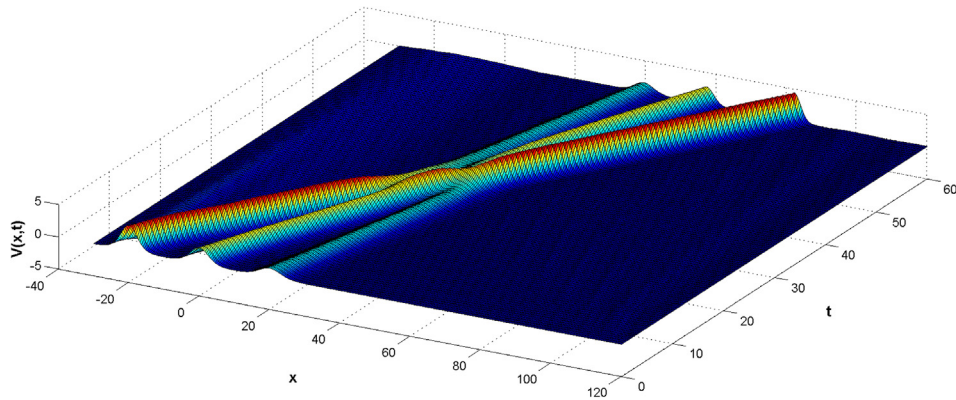


Fig. 3. Graphs of approximation solutions using the RBF-FD method with $\epsilon = 2$, $h = 1/10$, $n_s = 50$ and $\tau = 1/100$ for Example 3.

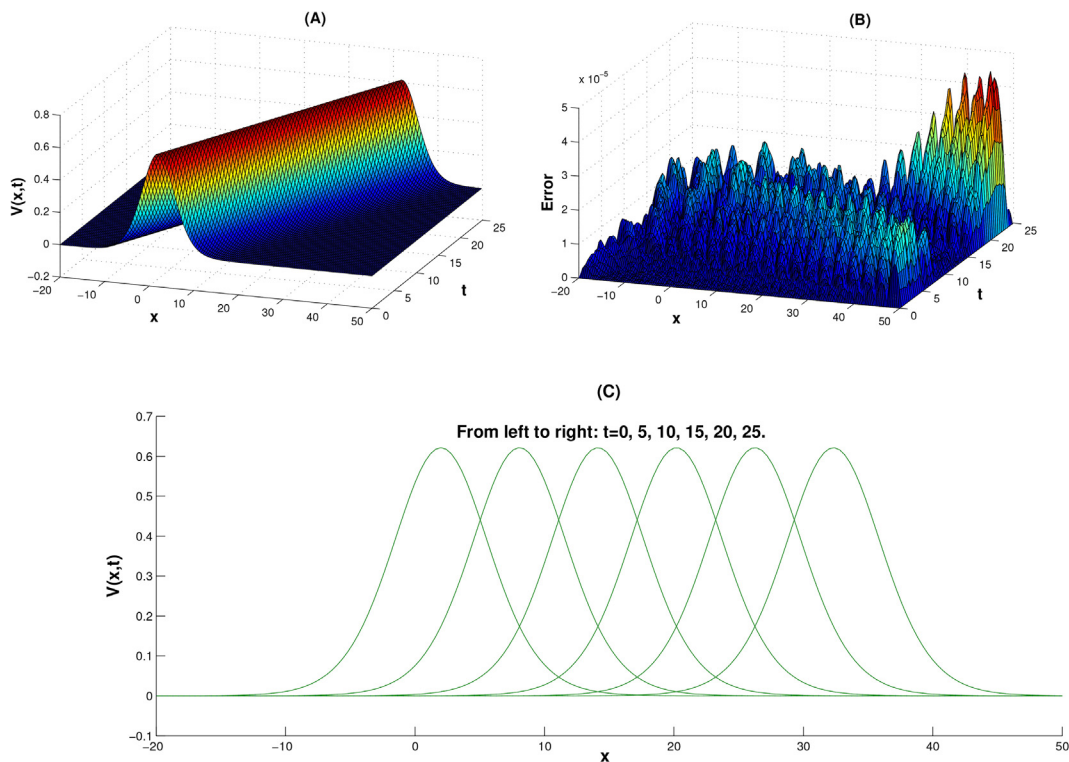


Fig. 4. Graphs of approximation solutions (A) and errors (B), and plots of $V(x, t)$ at $t = 0, 5, 10, 15, 20, 25$ (C), using the RBF-FD method with $\epsilon = 2$, $h = 1/10$, $n_s = 50$ and $\tau = 1/1000$ for Example 4.

Table 6Comparison of errors between RBF-FD and RBFs (Haq and Uddin, 2011) methods with $\tau = 0.001$, $h = 0.1$ and $n_s = 50$ for Example 4.

<i>t</i>	RBF-FD				RBFs			
	L_∞	L_2	I_1	I_2	L_∞	L_2	I_1	I_2
0.0	0.0000e – 00	0.0000e – 00	5.9736	1.2725	0.000e – 00	0.000e – 00	5.97361	1.27250
10	1.7305e – 05	7.4649e – 06	5.9737	1.2725	6.159e – 05	3.861e – 05	5.97363	1.27250
20	3.1814e – 05	1.0129e – 05	5.9738	1.2725	6.185e – 05	3.234e – 05	5.97381	1.27250
25	4.3371e – 05	1.4914e – 05	5.9727	1.2725	9.879e – 05	6.230e – 05	5.97280	1.27250

RBF method (Haq and Uddin, 2011) is equal to $1.5063e + 10$. Thus, the RBF-FD method is more well-conditioned than the RBF one. Therefore, these results verify an improvement of the RBF-FD method versus RBFs (Haq and Uddin, 2011) ones.

6. Conclusion

In this work, the stable computation for numerical solution of the Kawahara equations using collocation method based on RBF-FD has been presented. The stability analysis of the proposed method was proved analytically. The efficiency and accuracy were tested numerically by four examples and given some comparisons with some earlier works. The numerical results given in the previous section demonstrate a good accuracy of proposed method and an improvement versus the methods RBFs, CDQ and PDQ, and MCBC-DQM. In the linear system of the RBF-FD method, the sparse and n_s diagonal and well conditioned system matrices has been observed. So, the number of nodes can be increased to some extent. Moreover, this method is meshless.

Conflict of interest

The authors declare that there is no conflict of interest concerning the manuscript.

References

- Abazari, R., Soltanizadeh, B., 2012. Reduced differential transform method and its application on Kawahara equations. *Thai J. Math.* 11 (1), 199–216.
- Abbasbandy, S., 2010. Homotopy analysis method for the Kawahara equation. *Nonlinear Anal.: Real World Appl.* 11 (1), 307–312.
- Ablowitz, M.J., Ablowitz, M., Clarkson, P., Clarkson, P.A., 1991. Solitons, nonlinear evolution equations and inverse scattering, vol. 149. Cambridge University Press.
- Başhan, A., 2019. An efficient approximation to numerical solutions for the Kawahara equation via modified cubic B-Spline differential quadrature method. *Mediterr. J. Math.* 16 (1), 14.
- Başhan, A.A., 2019. mixed algorithm for numerical computation of soliton solutions of the coupled KdV equation: finite difference method and differential quadrature method. *Appl. Math. Comput.* 360, 42–57.
- Başhan, A., 2019. A novel approach via mixed Crank-Nicolson scheme and differential quadrature method for numerical solutions of solitons of mKdV equation. *Pramana-J. Phys.* 92 (6), 84.
- Başhan, A., Yagmurlu, N.M., Ucar, Y., Esen, A., 2017. An effective approach to numerical soliton solutions for the Schrödinger equation via modified cubic B-spline differential quadrature method. *Chaos, Solitons Fractals* 100, 45–56.
- Bayona, V., Moscoso, M., Carretero, M., Kindelan, M., 2010. RBF-FD formulas and convergence properties. *J. Comput. Phys.* 229 (22), 8281–8295.
- Bibi, N., Tirmizi, S.I.A., Haq, S., 2011. Meshless method of lines for numerical solution of Kawahara type equations. *Appl. Math.* 2 (05), 608.
- Ceballos, J.C., Sepulveda, M., Villagrán, O.P.V., 2007. The Korteweg-de Vries-Kawahara equation in a bounded domain and some numerical results. *Appl. Math. Comput.* 190 (1), 912–936.
- Dehghan, M., Abbaszadeh, M.A., 2017. local meshless method for solving multi-dimensional Vlasov-Poisson and Vlasov-Poisson-Fokker-Planck systems arising in plasma physics. *Eng. Comput.* 33 (4), 961–981.
- Dehghan, M., Mohammadi, V.A., 2017. numerical scheme based on radial basis function finite difference (RBF-FD) technique for solving the high-dimensional nonlinear Schrödinger equations using an explicit time discretization: Runge-Kutta method. *Comput. Phys. Commun.* 217, 23–34.
- Dereli, Y., Irk, D., Dağ, İ., 2009. Soliton solutions for NLS equation using radial basis functions. *Chaos, Solitons Fractals* 42 (2), 1227–1233.
- Djidjeli, K., Price, W.G., Twizell, E.H., Wang, Y., 1995. Numerical methods for the solution of the third-and fifth-order dispersive Korteweg-de Vries equations. *J. Comput. Appl. Math.* 58 (3), 307–336.
- Meshfree, Fasshauer G.E., 2007. Approximation Methods with Matlab:(With CD-ROM), vol. 6. World Scientific Publishing Co Inc.
- Gong, Y., Cai, J., Wang, Y., 2014. Multi-symplectic Fourier pseudospectral method for the Kawahara equation. *Commun. Comput. Phys.* 16 (1), 35–55.
- Haq, S., Uddin, M., 2011. RBFs approximation method for Kawahara equation. *Eng. Anal. Boundary Elem.* 35 (3), 575–580.
- Hussain, M., Haq, S., 2020. Numerical simulation of solitary waves of Rosenau–KdV equation by Crank–Nicolson meshless spectral interpolation method. *Eur. Phys. J. Plus* 135 (1), 98.
- Jeffrey, A., Xu, S., 1989. Travelling wave solutions to certain non-linear evolution equations. *Int. J. Non-Linear Mech.* 24 (5), 425–429.
- Karakoc, B.G., Zeybek, H., Ak, T., 2014. Numerical solutions of the Kawahara equation by the septic B-spline collocation method. *Stat., Optim. Inf. Comput.* 2 (3), 211–221.
- Kashkari, B.S., 2014. Application of optimal homotopy asymptotic method for the approximate solution of Kawahara equation. *Appl. Math. Sci.* 8 (18), 875–884.
- Korkmaz, A., Dağ, İ., 2009. Crank–Nicolson-differential quadrature algorithms for the Kawahara equation. *Chaos Solitons Fractals* 42 (1), 65–73.
- Martin, B., Fornberg, B., 2017. Using radial basis function-generated finite differences (RBF-FD) to solve heat transfer equilibrium problems in domains with interfaces. *Eng. Anal. Boundary Elem.* 79, 38–48.
- Micchelli, C.A., 1984. Interpolation of scattered data: distance matrices and conditionally positive definite functions. In: *Approximation Theory and Spline Functions*. Springer, pp. 143–145.
- Mohanty, R., Gopal, V., 2011. High accuracy cubic spline finite difference approximation for the solution of one-space dimensional non-linear wave equations. *Appl. Math. Comput.* 218 (8), 4234–4244.
- Mohanty, R.K., Khurana, G.A., 2019. new high accuracy cubic spline method based on half-step discretization for the system of 1D non-linear wave equations. *Eng. Comput.* 36 (3), 930–957.
- Mokhtari, R., Mohseni, M.A., 2012. meshless method for solving mKdV equation. *Comput. Phys. Commun.* 183 (6), 1259–1268.
- Nikan, O., Golbabai, A., Nikazad, T., 2019. Solitary wave solution of the nonlinear KdV-Benjamin-Bona-Mahony-Burgers model via two meshless methods. *Eur. Phys. J. Plus* 134 (7), 367.
- Nikan, O., Machado, J.T., Golbabai, A., Nikazad, T., 2019. Numerical investigation of the nonlinear modified anomalous diffusion process. *Nonlinear Dyn.* 97 (4), 2757–2775.
- Rashidinia, J., Rasoulizadeh, M.N., 2019. Numerical methods based on radial basis function-generated finite difference (RBF-FD) for solution of GKdVB equation. *Wave Motion* 90, 152–167.
- Raslan, K., EL-Danaf, T.S., 2010. Solitary waves solutions of the MRLW equation using quintic B-splines. *J. King Saud Univ.-Sci.* 22 (3), 161–166.
- Safdari-Vaighani, A., Mahzarnia, A., 2015. The evaluation of compound options based on RBF approximation methods. *Eng. Anal. Boundary Elem.* 58, 112–118.
- Sarra, S.A., 2005. Adaptive radial basis function methods for time dependent partial differential equations. *Appl. Numer. Math.* 54 (1), 79–94.
- Sharifi, S., Rashidinia, J., 2019. Collocation method for Convection-Reaction-Diffusion equation. *J. King Saud Univ.-Sci.* 31 (4), 1115–1121.
- Shechter, G., 2004. Matlab package kdtree.
- Sirendaoreji, 2004. New exact travelling wave solutions for the Kawahara and modified Kawahara equations. *Chaos Solitons Fractals* 19 (1), 147–150.
- Wang, Q., 2011. The optimal homotopy-analysis method for Kawahara equation. *Nonlinear Analysis: Real World Applications* 12 (3), 1555–1561.
- Wright, G.B., Fornberg, B., 2006. Scattered node compact finite difference-type formulas generated from radial basis functions. *J. Comput. Phys.* 212 (1), 99–123.
- Yamamoto, Y., Takizawa, É.I., 1981. On a solution on non-linear time-evolution equation of fifth order. *J. Phys. Soc. Jpn.* 50 (5), 1421–1422.
- Yusufoglu, E., Bekir, A., Alp, M., 2008. Periodic and solitary wave solutions of Kawahara and modified Kawahara equations by using Sine-Cosine method. *Chaos, Solitons Fractals* 37 (4), 1193–1197.